Carbohydrate Polymers 88 (2012) 179–184

Contents lists available at SciVerse ScienceDirect

Carbohydrate Polymers

journal homepage: www.elsevier.com/locate/carbpol

Hydrothermal fabrication, characterization, and biological activity of cellulose/$CaCO_3$ bionanocomposites

Ning Jia[a], Shu-Ming Li[a], Ming-Guo Ma[a,*], Run-Cang Sun[a,b], Jie-Fang Zhu[c]

[a] Institute of Biomass Chemistry and Technology, College of Materials Science and Technology, Beijing Forestry University, Beijing 100083, PR China
[b] State Key Laboratory of Pulp and Paper Engineering, South China University of Technology, Guangzhou 510640, PR China
[c] Department of Materials Chemistry, The Ångström Laboratory, Uppsala University, Uppsala 75121, Sweden

ARTICLE INFO

Article history:
Received 2 November 2011
Received in revised form
21 November 2011
Accepted 25 November 2011
Available online 6 December 2011

Keywords:
Cellulose
$CaCO_3$
Bionanocomposites
Hydrothermal
Biocompatibility

ABSTRACT

Bionanocomposites with the combination of natural polymers and inorganic nanoparticles may induce unique properties and exhibit promising functions for different applications. Herein, we report a hydrothermal route to the preparation of cellulose/$CaCO_3$ bionanocomposites using the cellulose solution, $Ca(NO_3)_2{\cdot}4H_2O$ and $Na_2SiO_3{\cdot}9H_2O$. The cellulose solution was previously prepared by the dissolution of microcrystalline cellulose in NaOH–urea aqueous solution. The urea also acts as the CO_3^{2-} source for the synthesis of $CaCO_3$. The influences of several reaction parameters, such as the heating time, the heating temperature, and the types of additives on the products were investigated by X-ray powder diffraction, Fourier transform infrared spectrometry, scanning electron microscopy, thermogravimetric analysis, and differential thermal analysis. The experimental results demonstrated that the hydrothermal conditions had an effect on the morphology of the bionanocomposites. Cytotoxicity experiments indicated that the cellulose/$CaCO_3$ bionanocomposites had good biocompatibility, so that the bionanocomposites could be ideal candidate for practical biomedical applications.

1. Introduction

Bionanocomposites that consist of natural polymers and inorganic nanoparticles have gained more interest as environmentally friendly and biofunctional materials due to its interesting properties such as biocompatibility, biodegradability and potential applications in optical, electrochemical, magnetic, catalytic, and biomedical fields (Alcantara, Aranda, Darder, & Ruiz-Hitzky, 2010; Darder, Aranda, & Ruiz-Hitzky, 2007; Luckarift, Dickerson, Sandhage, & Spain, 2006; Ruiz-Hitzky, Darder, Aranda, & Ariga, 2010; Ruiz-Hitzky, Darder, Aranda, del Burgo, & del Real, 2009). Until now, several successful strategies including drop-casting process (Biswas et al., 2010), ultraviolet irradiation reduction method (Shameli et al., 2010), grafting from approach (Habibi et al., 2008), casting/evaporation technique (Habibi & Dufresne, 2008), and solvent casting/particle leaching (Rezwan, Chen, Blaker, & Boccaccini, 2006) have been reported to prepare bionanocomposites such as chitosan/clay (Shchipunov, Ivanova, & Silant'ev, 2009), xanthan gum/sepiolite (Ruiz-Hitzky et al., 2009), and vanadium oxide/gelatin (Carn et al., 2010). Among of these bionanocomposites, the synthesis of cellulose-based bionanocomposites has attracted particular attention (Chen, Liu, Chang, Cao, & Anderson, 2009; Habibi & Dufresne, 2008; Rhim & Ng, 2007) because cellulose is one of the most abundant natural polymers and renewable resources on the earth (Eichhorn et al., 2010).

As the main inorganic component of human bone, teeth, and shells, hydroxyapatite [$Ca_{10}(PO_4)_6(OH)_2$, HA] and calcium carbonate ($CaCO_3$) are known to have biological activities of protein-adhesive properties, cell compatibility, and hard tissue compatibility (Hanein, Sabanay, Addadi, & Geiger, 1993; Hott, Noel, Bernache-Assolant, Rey, & Marie, 1997; Luo & Andrade, 1998; Ohgushi et al., 1992). Cellulose/HA bionanocomposites have been extensively explored (Hong et al., 2006; Wan et al., 2006; Zhang et al., 2009). It is possible that the composites of bioactive $CaCO_3$ with cellulose induce unique functional properties. However, there have been only few literatures reporting on the synthesis of cellulose/$CaCO_3$ bionanocomposites (Dalas, Klepetsanis, & Koutsoukos, 2000; Fimbel & Siffert, 1986; Shen, Song, Qian, & Yang, 2010; Subramanian, Maloney, & Paulapuro, 2005; Vilela et al., 2010). The research of the interaction of $CaCO_3$ (calcite) with cellulose fibers in aqueous medium was first reported in 1986 (Fimbel & Siffert, 1986). Then, Dalas et al. (2000) investigated the kinetics process of the calcium carbonate deposition on cellulose substrate. After that, the coprecipitation of calcium carbonate as filler in papermaking was reported (Subramanian et al., 2005). More recently, Vilela et al. (2010) prepared cellulose/$CaCO_3$

* Corresponding author. Tel.: +86 10 62336592; fax: +86 10 62336972.
E-mail address: mg_ma@bjfu.edu.cn (M.-G. Ma).

0144-8617/$ – see front matter © 2011 Elsevier Ltd. All rights reserved.
doi:10.1016/j.carbpol.2011.11.086

bionanocomposite by the controlled reaction of $CaCl_2$ with dimethylcarbonate ($(CH_3)_2CO_3$) in alkaline medium in the presence of cellulose fibers. To date, however, there has been no report on special discussion of cellulose/$CaCO_3$ bionanocomposites prepared by hydrothermal method, which provides unique temperature–pressure environments and has an advantage of controlling morphology of the products by adjusting the reaction parameters. In previous studies, we synthesized cellulose-carbonated HA bionanocomposites using cellulose solution, $CaCl_2$, and NaH_2PO_4 in aqueous solution by hydrothermal method at 180 °C for 24 h (Jia, Li, Ma, Sun, & Zhu, 2010).

Herein, we report the synthesis of the cellulose/$CaCO_3$ bionanocomposites by hydrothermal method using the cellulose solution, $Ca(NO_3)_2{\cdot}4H_2O$ solution, and $Na_2SiO_3{\cdot}9H_2O$ solution. The urea acts as both the additive for the dissolution of cellulose and the CO_3^{2-} source for the synthesis of $CaCO_3$. The biological activity of cellulose/$CaCO_3$ bionanocomposites was also studied by cytotoxicity experiments.

2. Experimental

2.1. Preparation of cellulose/$CaCO_3$ bionanocomposites

All chemicals were of analytical grade and used as received without further purification. All experiments were conducted under air atmosphere. The preparation of cellulose solution followed our previous report (Jia et al., 2010). In a typical synthesis, 7.00 g of NaOH and 12.00 g of urea were added into 81 mL of distilled water under vigorous stirring to form NaOH–urea aqueous solution. Then, 3.24 g of microcrystalline cellulose was added into the above solution under vigorous stirring. The above solution was cooled to −12 °C for 12 h. The obtained cellulose solution was used for the preparation of cellulose/$CaCO_3$ bionanocomposites.

For the synthesis of cellulose/$CaCO_3$ bionanocomposites, 5 mL of $Ca(NO_3)_2{\cdot}4H_2O$ solution (0.40 mol/L) and 5 mL of $Na_2SiO_3{\cdot}9H_2O$ solution (0.40 mol/L) were added into the above obtained cellulose solution (10 mL) under vigorous stir. The mixture solution was transferred into a 25-mL Teflon-lined stainless steel autoclave. The autoclave was maintained at a certain temperature for a certain time. The product was separated from the solution by centrifugation, washed by water and ethanol several times and dried at 60 °C for further characterization.

2.2. Characterization

X-ray powder diffraction (XRD) patterns were obtained in 2θ range from 10° to 70° on a X'Pert PRO MPD diffractometer operating at 40 kV with Cu Kα (λ = 1.5405 Å) radiation. Fourier transform infrared (FT-IR) spectroscopy was carried out on an FT-IR spectrophotometer (Nicolet 510), using the KBr disk method. Scanning electron microscopy (SEM) images were recorded with a Hitachi 3400N scanning electron microscopy. All samples were Au coated prior to examination by SEM. Thermal behavior of the samples was tested using thermogravimetric analysis (TGA) and differential thermal analysis (DTA) on a simultaneous thermal analyzer (DTG-60, Shimadzu) at a heating rate of 10 °C min^{-1} in flowing air.

2.3. Cell cytotoxicity

The human gastric carcinoma cells (MGC-803) that were cultured in an RPMI-1640 medium supplemented with 10% FBS (fetal bovine serum) and 1% penicillin–streptomycin at 37 °C for 48 h, were used for cell viability test. Then, the cells were seeded in 96-well flat-bottom microassay plates at a concentration of 1×10^4 cells/mL and cultured for 24 h. The sterilized samples (the cellulose/$CaCO_3$ bionanocomposites) were added into wells at the concentration from 10, 20, 30, 50 to 100 μg/mL, and were co-cultured with cells for 48 h. The sample free tissue culture plate was used as a control. Cell viability was quantified by MTT (3-(4.5-dimethylthiazol-2-yl)-2,5-diphenyltetrazolium bromide) assay. Data are representative as mean value of five parallel experiments.

3. Results and discussion

3.1. The phase, microstructure, and morphologies of the cellulose/$CaCO_3$ bionanocomposites

The phase of the cellulose/$CaCO_3$ bionanocomposites was characterized by XRD, as shown in Fig. 1. The pattern of the sample prepared by hydrothermal method at 160 °C for 24 h indicated the existence of the mixed phases of cellulose and $CaCO_3$: cellulose (2θ = 20.0° and 21.9°) and calcite (marked with C in Fig. 1e). This result shows the successfully preparation of cellulose/$CaCO_3$ bionanocomposites. The solubility product (K_{sp}) of $CaCO_3$ is 2.8×10^{-9}, which is smaller than that of $CaSiO_3$ (2.5×10^{-8}). As we all know, the product is first obtained with low K_{sp} value under normal condition. Therefore, the obtained products are not the cellulose/$CaSiO_3$ bionanocomposites, but cellulose/$CaCO_3$ bionanocomposites. There is still existence of a small amount of aragonite. As we know, aragonite is the metastable phase of $CaCO_3$, while calcite is the thermodynamically stable phase of $CaCO_3$. This phenomenon might be explained by the part formation of aragonite in the bionanocomposites, and then the aragonite was converted to the calcite after long time reaction. The phases of the samples synthesized at 160 °C for 2 h, 4 h, 6 h, and 12 h were also investigated (Fig. 1a–d). One can see that all of the samples have similar XRD patterns. However, the peak intensity of aragonite decreased with increasing heating time, further implying the conversion from the metastable aragonite to the thermodynamically stable calcite. Some groups (Hosoda, Sugawara, & Kato, 2003; Lakshminarayanan, Valiyaveettil, & Loy, 2003; Ogomi, Serizawa, & Akashi, 2005; Serizawa, Tateishi, & Akashi, 2003) have found the similar phenomenon on the synthesis of poly(vinyl alcohol)/$CaCO_3$ composite and thought that poly(vinyl alcohol) might affect the conversion of aragonite. Herein, we used cellulose as matrix, which

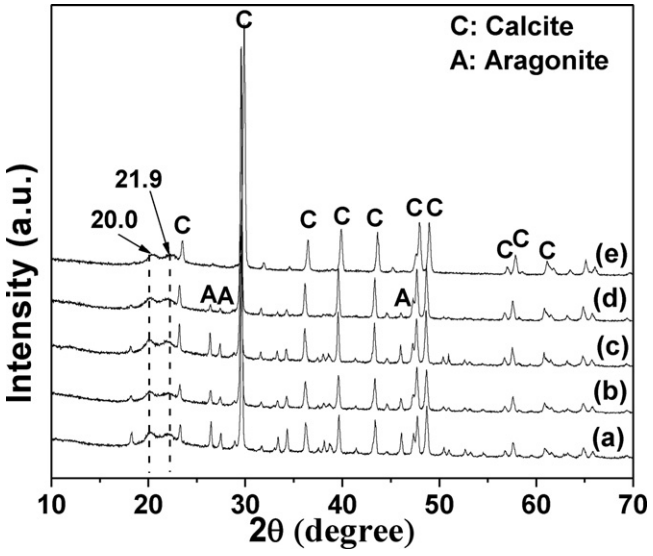

Fig. 1. XRD patterns of the cellulose/$CaCO_3$ bionanocomposites prepared by hydrothermal method at 160 °C for different times: (a) 2 h; (b) 4 h; (c) 6 h; (d) 12 h; and (e) 24 h.

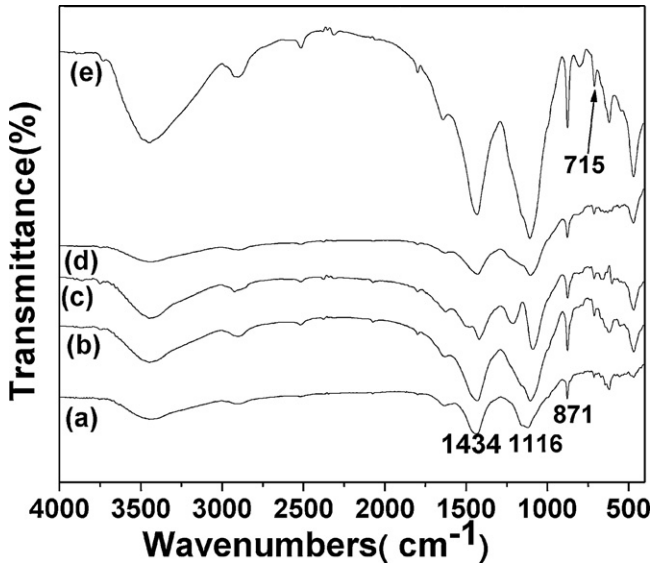

Fig. 2. FT-IR spectra of the cellulose/$CaCO_3$ bionanocomposites prepared by hydrothermal method at 160 °C for different times: (a) 2 h; (b) 4 h; (c) 6 h; (d) 12 h; and (e) 24 h.

might also influence the conversion from aragonite to calcite. Of course, the intrinsic formation mechanism of $CaCO_3$ polymorph needs to be further explored.

The crystal structure and phase of the bionanocomposites were further examined by FT-IR analysis, as shown in Fig. 2. The FT-IR spectra of all the obtained bionanocomposites showed the typical bands of cellulose at 1116 cm^{-1} (the C—O in cellulose) and $CaCO_3$ at around 1434 cm^{-1} (ν_{3-3} CO_3^{2-} and ν_{3-4} CO_3^{2-}) (He, Huang, Liu, Chen, & Xu, 2007; Nelson & Featherstone, 1982). The cellulose/$CaCO_3$ bionanocomposites exhibit crystalline bands at 715 cm^{-1} and 871 cm^{-1} assignable to calcite (Donners et al., 2000). However, the typical band of aragonite around 855 cm^{-1} was not observed, probably due to its too small amount under the detect limitation (D'Souza et al., 1999; Naka, Keum, Tanaka, & Chujo, 2000). In addition, the peak intensity of cellulose/$CaCO_3$ bionanocomposites prepared for 24 h was stronger than those of the others, indicating better crystallization and the transform from aragonite to calcite. These results were consistent with the XRD results.

The morphologies and microstructures of the cellulose/$CaCO_3$ bionanocomposites were investigated by SEM. The SEM images of the sample that was synthesized using cellulose solution, were shown in Fig. 3c and d. One can see that the $CaCO_3$ congregates and grows on cellulose as substrate (Fig. 3c). Magnified micrograph of the bionanocomposites was shown in Fig. 3d. The size of the $CaCO_3$ congregates was around 250 nm. Interestingly, pores were observed around the center of $CaCO_3$ congregates, indicating that the $CaCO_3$ congregates may be assembled from nanoparticles. For comparison, using microcrystalline cellulose instead of cellulose solution, the SEM images of the sample were shown in Fig. 3a and b. One can see the cellulose with fiber-like morphology (Fig. 3a). Irregular particles were observed on the surface of cellulose (Fig. 3b). These experimental results indicated that the NaOH/urea solution decreased the size of fiber-like cellulose and favored the formation of $CaCO_3$ and thus the composite of cellulose and $CaCO_3$. Irregular polyhedral $CaCO_3$ embedded in the cellulose matrix was observed without $Na_2SiO_3{\cdot}9H_2O$ solution (Fig. 3e). Magnified micrograph of the irregular polyhedral $CaCO_3$ was shown in Fig. 3f, which is completely different morphology compared to Fig. 3c and d, indicating that the addition of $Na_2SiO_3{\cdot}9H_2O$ solution played an important role in the control of the morphology of $CaCO_3$ in bionanocomposites.

3.2. The influences of heating time, heating temperature, and additives

We also investigated the effect of heating time on the morphologies of the samples. When heating time was 2 h, the $CaCO_3$ particles dispersed in the cellulose matrix were observed (Fig. 4a). Increasing the heating time to 4 h, the morphology did not change (Fig. 4b). However, when the heating time increased to 6 h, the $CaCO_3$ aggregation and growth were observed, as shown in Fig. 4c and d. Magnified micrograph of the $CaCO_3$ agglomerates was shown in Fig. 4d, from which one can see the $CaCO_3$ agglomerates consisted of irregular nanoparticles. When the heating time was increased to 12 h, the porous structure in $CaCO_3$ agglomerates appeared (Fig. 4e and f), indicating the further aggregation of $CaCO_3$. From Figs. 3 and 4, one can see the morphology evolution process of $CaCO_3$ in the cellulose matrix, indicating that the heating time had an effect on the shape and microstructure of the cellulose/$CaCO_3$ bionanocomposites. The fabrication of the cellulose/$CaCO_3$ bionanocomposites involved the nucleation, growth, ripening, and agglomeration processes. The longer heating time favored the

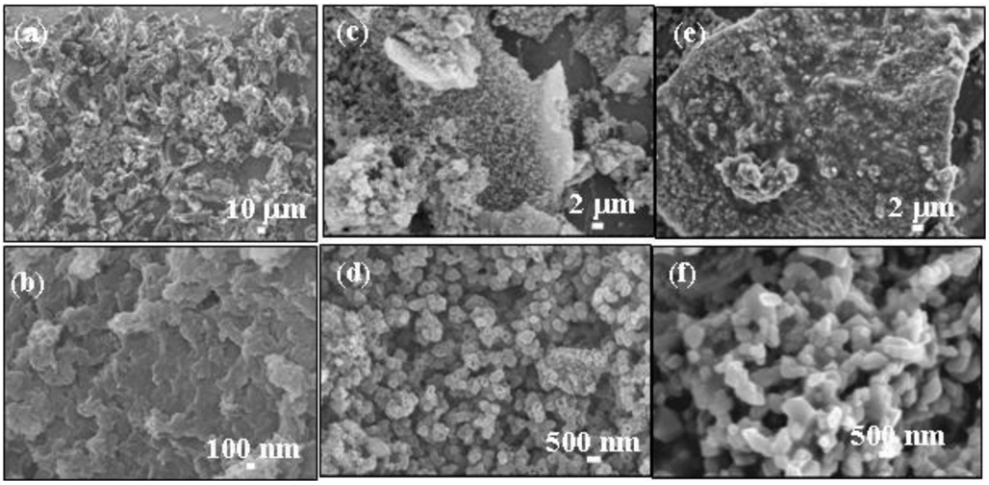

Fig. 3. SEM images of the cellulose/$CaCO_3$ bionanocomposites prepared by hydrothermal method at 160 °C for 24 h: (a and b) using microcrystalline cellulose; (c and d) using cellulose solution, (e and f) without $Na_2SiO_3{\cdot}9H_2O$ solution.

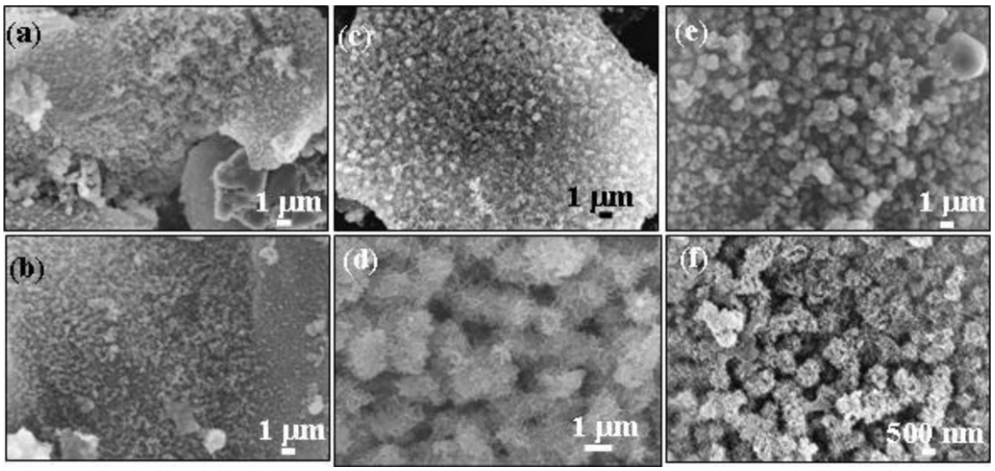

Fig. 4. SEM images of the cellulose/$CaCO_3$ bionanocomposites prepared by hydrothermal method at 160 °C for different times: (a) 2 h; (b) 4 h; (c and d) 6 h; and (e and f) 12 h.

aggregation of $CaCO_3$ and induced the formation of the porous structure in $CaCO_3$ agglomerates.

Investigation has been conducted on the effect of the heating temperature on the cellulose/$CaCO_3$ bionanocomposites. The cellulose/$CaCO_3$ bionanocomposites were also prepared at 120 °C and 180 °C for 24 h, respectively, while other reaction conditions were kept the same. Fig. 5 shows the corresponding SEM images of the cellulose/$CaCO_3$ bionanocomposites prepared at different temperatures. When the heating temperature was decreased to 120 °C, no significant differences were observed on the morphology of the cellulose/$CaCO_3$ bionanocomposites (Fig. 5a–c), compared to Fig. 3. A slight difference is that no apparent porous structure in $CaCO_3$ congregates was observed. When the heating temperature was increased to 180 °C, no $CaCO_3$ congregates were observed (Fig. 5d and e). These results implied that the heating temperature had an influence on the morphology of cellulose/$CaCO_3$ bionanocomposites. As we all know, the higher heating temperature led to a fast nucleation. Then the nuclei grew to form particles and fast growth was restrained. With the elevation of temperature, the small particles were obtained and no congregates were observed.

The influences of the additives such as cetyltrimethyl ammonium bromide (CTAB), sodium dodecyl benzene sulfonate (SDBS), and LiCl/*N*,*N*-dimethylacetamide on the morphologies of bionanocomposites were investigated, as shown in Fig. 6. When CTAB was used as additive, the similar shapes were obtained (Fig. 6a and b). When SDBS was used as additive, the size of congregates decreased (Fig. 6c and d). When the LiCl/*N*,*N*-dimethylacetamide solution instead of NaOH/urea solution was used, particles and spheres were observed on the surface of cellulose fibers (Fig. 6e and f). These results indicated that the additive species had an influence on the shape and size of $CaCO_3$ in bionanocomposites which probably is also related to the change of CO_3^{2-} source. The different crystal facets have different growth rates. The different additive had different adsorption ability on various facets, leading to the different growth rate for different crystal facet and the synthesis of different morphologies in bionanocomposites.

3.3. The thermal stability of the cellulose/$CaCO_3$ bionanocomposites

The thermal stability of the cellulose/$CaCO_3$ bionanocomposites was also investigated by TGA and DTA. TGA and DTA curves for the prepared bionanocomposites at 160 °C for 2 h, 12 h, and 24 h are shown in Fig. 7, respectively. The TGA curves of the cellulose/$CaCO_3$ bionanocomposites exhibit a small weight loss in the region from room-temperature to 150 °C due to the loss of adsorbed water molecules, which come from the ambient environment, and this weight loss is accompanied by endothermic peaks at about 55 °C in the DTA curves. From TGA curves, it is observed that the weight loss takes places at two stages: the first one (from 250 °C to 350 °C)

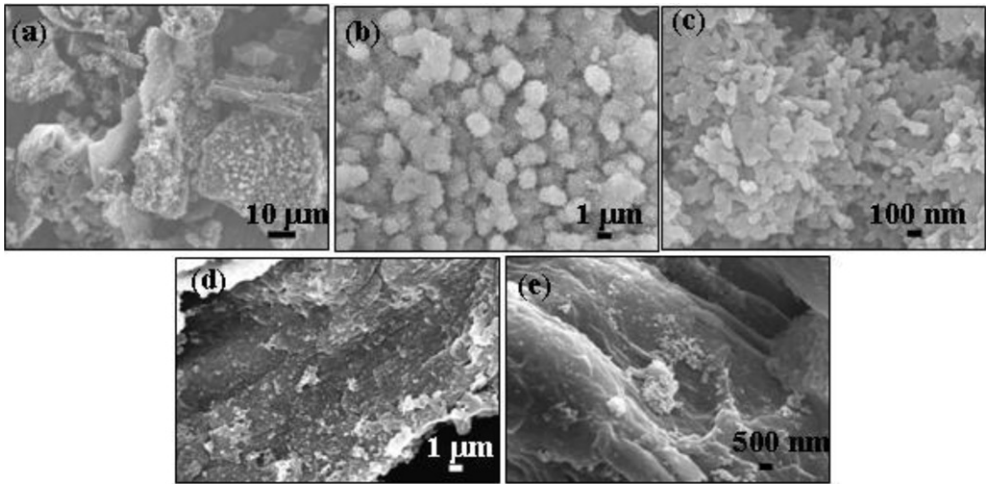

Fig. 5. SEM images of the cellulose/$CaCO_3$ bionanocomposites prepared by hydrothermal method at different temperatures for 24 h: (a–c) 120 °C and (d and e) 180 °C.

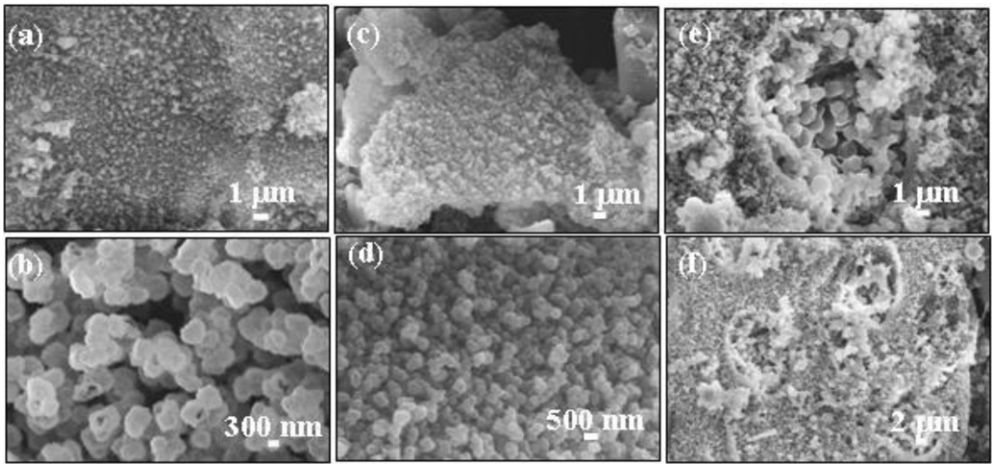

Fig. 6. SEM images of the cellulose/$CaCO_3$ bionanocomposites prepared by hydrothermal method at 160 °C for 24 h using different additives: (a and b) CTAB; (c and d) SDBS; and (e and f) LiCl/*N*,*N*-dimethylacetamide.

is probably caused by thermal degradation, and the other (from 350 °C to 500 °C) is probably caused by the complete decomposition of cellulose and $CaCO_3$ in bionanocomposites (Zheng, Zhou, Du, & Zhang, 2002). The obvious weight losses of the cellulose/$CaCO_3$ bionanocomposites prepared at 160 °C for 2 h, 12 h, and 24 h were ~46.8%, 43.4%, and 47.3% from 200 °C to 544 °C in the TGA curves, respectively. One can clearly see the corresponding exothermic peaks at about 329 °C, 425 °C, and 490 °C in the DTA curves, testifying that the TGA profiles are in good agreement with the DTA results of these bionanocomposites.

3.4. Cell cytotoxicity of the cellulose/$CaCO_3$ bionanocomposites

Cell cytotoxicity of the cellulose/$CaCO_3$ bionanocomposites is very important for their application as biomedical materials. In synthesis system, NaOH, urea, $Ca(NO_3)_2{\cdot}4H_2O$ and $Na_2SiO_3{\cdot}9H_2O$ were used as reactants, which have almost no biological toxicity, and thus they are biologically safe. Therefore, it is expected that the cellulose/$CaCO_3$ bionanocomposite was biologically compatible. Mesenchymal stem cells (MSCs) are multipotent stem cells that can differentiate into a variety of cell types and are widely used as seed cells in tissue engineering. A 5-dimethylthiazol-2-yl-2,5-diphenyltetrazolium bromide (MTT) assay was performed, which was a simple colorimetric assay to measure cell cytotoxicity. In this study the typical cellulose/$CaCO_3$ bionanocomposites synthesized using the cellulose solution were compared with reference tissue culture plates in terms of in vitro cytotoxicity using MSCs (Fig. 8b). When the cellulose/$CaCO_3$ bionanocomposite concentration was 10 μg/mL, the cell viability value was 78.8%. From Fig. 8b, one can clearly see that even though the concentration of the cellulose/$CaCO_3$ bionanocomposites increased from 10 to 100 μg/mL after incubation for 48 h, the cell viability value was still 74.3% and a reduction of 25.7% in cellular viability was observed. For comparison, the cell cytotoxicity of cellulose/$CaCO_3$ bionanocomposites synthesized using the microcrystalline cellulose is shown in Fig. 8a. When the cellulose/$CaCO_3$ bionanocomposite concentrations were 10, 20, 30, 50, and 100 μg/mL, the cell viability values were 85.8, 94.8, 92.9, 88.7, and 85.8, respectively, which are more than those of the cellulose/$CaCO_3$ bionanocomposites synthesized using the cellulose solution. These results indicated that the cellulose/$CaCO_3$ bionanocomposite had essentially no in vitro cytotoxicity and was comparable with the tissue culture plates.

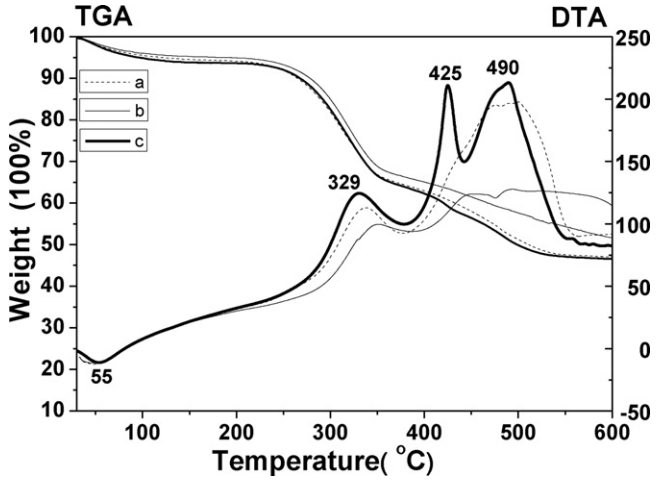

Fig. 7. TGA and DTA curves of the cellulose/$CaCO_3$ bionanocomposites prepared by hydrothermal method at 160 °C for different times: (a) 2 h; (b) 12 h; and (c) 24 h.

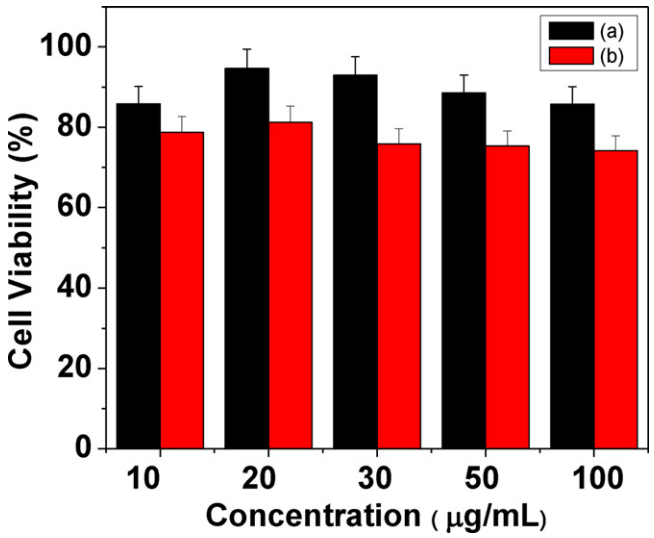

Fig. 8. Viabilities of normal human fibroblasts incubated with the cellulose/$CaCO_3$ bionanocomposites: (a) using microcrystalline cellulose and (b) using cellulose solution. They were determined by survival cells per well relative to that of untreated cells. The error bars stand for standard deviations.

4. Conclusions

In summary, we report the synthesis of the cellulose/$CaCO_3$ bionanocomposites using hydrothermal method by mixing the cellulose solution, $Ca(NO_3)_2{\cdot}4H_2O$ solution and $Na_2SiO_3{\cdot}9H_2O$ solution. The cellulose solution was previously prepared by the dissolution of microcrystalline cellulose in NaOH–urea aqueous solution. The urea acts as the CO_3^{2-} source for the synthesis of $CaCO_3$. XRD and FT-IR results indicated that the cellulose and calcite were obtained in bionanocomposites. SEM micrographs indicated that the $CaCO_3$ congregates with porous structure were dispersed in the cellulose matrix. The heating time, heating temperature and use of additive ($Na_2SiO_3{\cdot}9H_2O$) played an important role in the shape and microstructure of $CaCO_3$ in bionanocomposites. Cytotoxicity experiments indicated that the cellulose/$CaCO_3$ bionanocomposites had good biocompatibility. This synthetic strategy reported here opens a new window to the high value-added applications of cellulose.

Acknowledgments

Financial supports by the National Natural Science Foundation of China (31070511), Ångpanneföreningen's Foundation for Research and Development (Ref. no. 09-370), Miljöfonden from The Swedish Association of Graduate Engineers, and Major State Basic Research Development Program of China (973 Program) (No. 2010CB732204) are gratefully acknowledged.

References

Alcantara, A. C. S., Aranda, P., Darder, M., & Ruiz-Hitzky, E. (2010). Bionanocomposites based on alginate-zein/layered double hydroxide materials as drug delivery systems. *Journal of Materials Chemistry*, *20*, 9495–9504.

Biswas, A., Bayer, I. S., Zhao, H., Wang, T., Watanabe, F., & Biris, A. S. (2010). Design and synthesis of biomimetic multicomponent all-bone-minerals bionanocomposites. *Biomacromolecules*, *11*, 2545–2549.

Carn, F., Durupthy, O., Fayolle, B., Coradin, T., Mosser, G., Schmutz, M., et al. (2010). Assembling vanadium(V) oxide and gelatin into novel bionanocomposites with unexpected rubber-like properties. *Chemistry of Materials*, *22*, 398–408.

Chen, Y., Liu, C. H., Chang, P. R., Cao, X. D., & Anderson, D. P. (2009). Bionanocomposites based on pea starch and cellulose nanowhiskers hydrolyzed from pea hull fibre: Effect of hydrolysis time. *Carbohydrate Polymers*, *76*, 607–615.

Dalas, E., Klepetsanis, P. G., & Koutsoukos, P. G. (2000). Calcium carbonate deposition on cellulose. *Journal of Colloid Interface Science*, *224*, 56–62.

Darder, M., Aranda, P., & Ruiz-Hitzky, E. (2007). Bionanocomposites: A new concept of ecological, bioinspired, and functional hybrid materials. *Advanced Materials*, *19*, 1309–1319.

Donners, J. J. J. M., Heywood, B. R., Meijier, E. W., Nolte, R. J. M., Roman, C., Schenning, A. P. H. J., et al. (2000). Amorphus calcium carbonate stabilized by poly(propylene imine) dendrimers. *Chemical Communications*, 1937–1938.

D'Souza, S. M., Alexander, C., Carr, S. W., Waller, A. M., Whitcombe, M. J., & Vulfson, E. N. (1999). Directed nucleation of calcite at a crystal-imprinted polymer surface. *Nature*, *398*.

Eichhorn, S. J., Dufresne, A., Aranguren, M., Marcovich, N. E., Capadona, J. R., Rowan, S. J., et al. (2010). Review: Current international research into cellulose nanofibres and nanocomposites. *Journal of Materials Science*, *45*, 1–33.

Fimbel, P., & Siffert, B. (1986). Interaction of calcium carbonate (calcite) with cellulose fibres in aqueous medium. *Colloids and Surfaces*, *20*, 1–16.

Habibi, Y., & Dufresne, A. (2008). Highly filled bionanocomposites from functionalized polysaccharide nanocrystals. *Biomacromolecules*, *9*, 1974–1980.

Habibi, Y., Goffin, A. L., Schiltz, N., Duquesne, E., Dubois, P., & Dufresne, A. (2008). Bionanocomposites based on poly(epsilon-caprolactone)-grafted cellulose nanocrystals by ring-opening polymerization. *Journal of Materials Chemistry*, *18*, 5002–5010.

Hanein, D., Sabanay, H., Addadi, L., & Geiger, B. (1993). Selective interactions of cells with crystal surface: Implications for the mechanism cell adhesion. *Journal of Cell Science*, *104*, 275–288.

He, Q., Huang, Z., Liu, Y., Chen, W., & Xu, T. (2007). Template-directed one-step synthesis of flowerlike porous carbonated hydroxyapatite spheres. *Materials Letters*, *61*, 141–143.

Hong, L., Wang, Y. L., Jia, S. R., Huang, Y., Gao, C., & Wan, Y. Z. (2006). Hydroxyapatite/bacterial cellulose composites synthesized via a biomimetic route. *Materials Letters*, *60*, 1710–1713.

Hosoda, N., Sugawara, A., & Kato, T. (2003). Template effect of crystalline poly(vinyl alcohol) for selective formation of aragonite and vaterite $CaCO_3$ thin films. *Macromolecules*, *36*.

Hott, M., Noel, B., Bernache-Assolant, D., Rey, C., & Marie, P. J. (1997). Proliferation and differentiation of human trabecular osteoblastic cells on hydroxyapatite. *Journal of Biomedical Materials Research*, *37*, 508–516.

Jia, N., Li, S. M., Ma, M. G., Sun, R. C., & Zhu, J. F. (2010). Hydrothermal synthesis and characterization of cellulose-carbonated hydroxyapatite nanocomposites in NaOH–urea aqueous solution. *Science of Advanced Materials*, *2*, 210–214.

Lakshminarayanan, R., Valiyaveettil, S., & Loy, G. L. (2003). Selective nucleation of calcium carbonate polymorphs: Role of surface functionalization and poly(vinyl alcohol) additive. *Crystal Growth and Design*, *3*, 953–958.

Luckarift, H. R., Dickerson, M. B., Sandhage, K. H., & Spain, J. C. (2006). Rapid, room-temperature synthesis of antibacterial bionanocomposites of lysozyme with amorphous silica or titania. *Small*, *2*, 640–643.

Luo, Q., & Andrade, J. D. (1998). Cooperative adsorption of proteins onto hydroxyapatite. *Journal of Colloid Interface Science*, *200*, 104–113.

Naka, K., Keum, D. K., Tanaka, Y., & Chujo, Y. (2000). Control of crystal polymorphs by a 'latent inductor': Crystallization of calcium carbonate in conjunction with in situ radical polymerization of sodium acrylate in aqueous solution. *Chemical Communications*, 1537–1538.

Nelson, D. G. A., & Featherstone, J. D. B. (1982). Preparation, analysis, and characterization of carbonated apatites. *Calcified Tissue International*, *34*, 69–81.

Ogomi, D., Serizawa, T., & Akashi, M. (2005). Controlled release based on the dissolution of a calcium carbonate layer deposited on hydrogels. *Journal of Controlled Release*, *103*, 315–323.

Ohgushi, H., Okamura, M., Yoshikawa, T., Inoue, K., Senpuku, N., & Tamai, K. (1992). Bone formation process in porous calcium carbonate and hydroxyapatie. *Journal of Biomedical Materials Research*, *26*, 885–895.

Rezwan, K., Chen, Q. Z., Blaker, J. J., & Boccaccini, A. R. (2006). Biodegradable and bioactive porous polymer/inorganic composite scaffolds for bone tissue engineering. *Biomaterials*, *27*, 3413–3431.

Rhim, J. W., & Ng, P. K. W. (2007). Natural biopolymer-based nanocomposite films for packaging applications. *Critical Reviews in Food Science and Nutrition*, *47*, 411–433.

Ruiz-Hitzky, E., Darder, M., Aranda, P., & Ariga, K. (2010). Advances in biomimetic and nanostructured biohybrid materials. *Advanced Materials*, *22*, 323–336.

Ruiz-Hitzky, E., Darder, M., Aranda, P., del Burgo, M. A. M., & del Real, G. (2009). Bionanocomposites as new carriers for influenza vaccines. *Advanced Materials*, *21*, 4167–4171.

Serizawa, T., Tateishi, T., & Akashi, M. (2003). Cell-compatible properties of calcium carbonates and hydroxyapatite deposited on ultrathin poly(vinyl alcohol)-coated polyethylene films. *Journal of Biomaterials Science: Polymer Edition*, *14*, 653–663.

Shameli, K., Ahmad, M. B., Yunus, W. M. Z. W., Rustaiyan, A., Ibrahim, N. A., Zargar, M., et al. (2010). Green synthesis of silver/montmorillonite/chitosan bionanocomposites using the UV irradiation method and evaluation of antibacterial activity. *International Journal of Nanomedicine*, *5*, 875–887.

Shchipunov, Y., Ivanova, N., & Silant'ev, V. (2009). Bionanocomposites formed by in situ charged chitosan with clay. *Green Chemistry*, *11*, 1758–1761.

Shen, J., Song, Z. Q., Qian, X. R., & Yang, F. (2010). Carboxymethyl cellulose/alum modified precipitated calcium carbonate fillers: Preparation and their use in papermaking. *Carbohydrate Polymers*, *81*, 545–553.

Subramanian, R., Maloney, T., & Paulapuro, H. (2005). Calcium carbonate composite fillers. *Tappi Journal*, *4*, 23–27.

Vilela, C., Freire, C. S. R., Marques, P. A. A. P., Trindade, T., Neto, C. P., & Fardim, P. (2010). Synthesis and characterization of new $CaCO_3$/cellulose nanocomposites prepared by controlled hydrolysis of dimethylcarbonate. *Carbohydrate Polymers*, *79*, 1150–1156.

Wan, Y. Z., Hong, L., Jia, S. R., Huang, Y., Zhu, Y., Wang, Y. L., et al. (2006). Synthesis and characterization of hydroxyapatite-bacterial cellulose nanocomposites. *Composites Science and Technology*, *66*, 1825–1832.

Zhang, S. N., Xiong, G. Y., He, F., Huang, Y., Wang, Y. L., & Wan, Y. Z. (2009). Characterisation of hydroxyapatite/bacterial cellulose nanocomposites. *Polymers and Polymer Composites*, *17*, 353–358.

Zheng, H., Zhou, J., Du, Y., & Zhang, L. (2002). Cellulose/chitin films blended in NaOH/urea aqueous solution. *Journal of Applied Polymer Science*, *86*, 1679–1683.